EphB receptor forward signaling regulates area-specific reciprocal thalamic and cortical axon pathfinding

Michael A. Robichaux[a,b], George Chenaux[b,c], Hsin-Yi Henry Ho[d], Michael J. Soskis[d], Christopher Dravis[c], Kenneth Y. Kwan[e], Nenad Šestan[e], Michael Eldon Greenberg[d,1], Mark Henkemeyer[c,2], and Christopher W. Cowan[a,b,1,2]

[a]Department of Psychiatry, Harvard Medical School, McLean Hospital, Belmont, MA 02478; Departments of [b]Psychiatry and [c]Developmental Biology, The University of Texas Southwestern Medical Center, Dallas, TX 75390; [d]Department of Neurobiology, Harvard Medical School, Boston, MA 02115; and [e]Department of Neurobiology and Kavli Institute for Neuroscience, Yale University School of Medicine, New Haven, CT 06510

Contributed by Michael Eldon Greenberg, December 30, 2013 (sent for review October 27, 2013)

In early brain development, ascending thalamocortical axons (TCAs) navigate through the ventral telencephalon (VTel) to reach their target regions in the young cerebral cortex. Descending, deep-layer cortical axons subsequently target appropriate thalamic and subcortical target regions. However, precisely how and when corticothalamic axons (CTAs) identify their appropriate, reciprocal thalamic targets remains unclear. We show here that EphB1 and EphB2 receptors control proper navigation of a subset of TCA and CTA projections through the VTel. We show in vivo that EphB receptor forward signaling and the ephrinB1 ligand are required during the early navigation of L1-CAM$^+$ thalamic fibers in the VTel, and that the misguided thalamic fibers in *EphB1/2* KO mice appear to interact with cortical subregion-specific axon populations during reciprocal cortical axon guidance. As such, our findings suggest that descending cortical axons identify specific TCA subpopulations in the dorsal VTel to coordinate reciprocal cortical–thalamic connectivity in the early developing brain.

In the developing mammalian brain, proper neural circuitry between the thalamus and cerebral cortex is established through complex axon guidance processes (reviewed in refs. 1 and 2). The reciprocal cortical and thalamic fiber pathways establish critical circuits in the forebrain that mediate sensory processing and motor output (3). During embryonic brain development (~E11.5–E12.5), pioneer thalamocortical axon (TCA) fibers grow through the prethalamus before making a sharp turn past the diencephalic–telencephalic border (DTB) and into the ventral-most aspect of the ventral telencephalon (VTel), or subpallium, where they establish the internal capsule (IC). TCAs continue to ascend through the VTel toward the developing cortical plate and cross the pallial-subpallial border to reach the cortical intermediate zone (IZ) by age E13.5 (4). At these early ages, the developing VTel comprises the medial and lateral ganglionic eminences and globus pallidus, which together function as intermediate targets for TCA pathfinding and several axon guidance ligands and receptors (5–8) mediate proper guidance.

Descending cortical axons first navigate into the VTel around age E13.5, 1 d after TCA emergence into the ventral-most aspects of the VTel (4, 9, 10). Initially, the corticofugal axon (CFA) and corticothalamic axon (CTA) projections, from cortical layers V and VI, respectively, grow together into the IC, but then diverge. CTAs turn dorsally into the thalamus, whereas most of the CFAs continue into the ventral cerebral peduncle fiber bundle *en route* to lower brain targets (2). Before the development of these mature axon tracts, however, descending pioneer cortical fibers from the developing cortical subplate extend in the same physical space as ascending TCA fibers, and these opposing pathways have been demonstrated to cofasciculate with each other within the VTel (4, 11, 12). The "handshake hypothesis" proposed that TCAs navigate to their appropriate cortical regions by cofasciculating with reciprocal descending cortical axons encountered near the pallial–subpallial boundary (11, 13, 14); however, the functional importance of the handshake has remained controversial (15).

Eph receptors and ephrins have several functions in the development of the mammalian nervous system, including the proper navigation of axon growth cones (16–18). The Eph family of receptor tyrosine kinases is divided into two subgroups: the A class (A1–A8 and A10) and the B class (B1–B4 and B6), based largely on their similarity and binding preferences for ephrinA and ephrinB ligands (17). The high affinity interaction between Ephs and ephrins, typically upon cell–cell contact, triggers both forward and reverse signaling events that promote reorganization of the F-actin cytoskeleton (16, 19, 20), a cellular process critical for axon turning, outgrowth, and cell migration.

Using a variety of mouse genetic approaches, we show here that EphB1 and EphB2 receptor forward signaling, working together with the ephrinB1 ligand, is required for the proper reciprocal navigation of a subset of TCA and CTA fibers in the developing mouse brain. Our findings suggest that descending cortical axons selectively cofasciculate with specific TCA subpopulations to coordinate reciprocal cortical–thalamic connectivity in early brain development.

Results

EphB1 and EphB2 Receptors Regulate Axon Guidance in the VTel. EphB1 and EphB2 receptors are both expressed in the developing cortex (21, 22). To test their role in cortical axon guidance, we assessed L1-cell adhesion molecule+ (L1-CAM$^+$) axons traversing the VTel in wild-type (WT), *EphB1*$^{-/-}$, *EphB2*$^{-/-}$, and *EphB1/2* double knockout (*DKO*) (*EphB1*$^{-/-}$

Significance

In this study, we report a critical role of EphB forward signaling in proper thalamocortical axon guidance. Moreover, our findings provide support for the controversial "handshake hypothesis," which proposed that cofasciculation of specific thalamic and cortical axons controls proper cortical and thalamic interconnectivity. Finally, growing evidence suggests cortical synaptic connectivity and white matter tract development are abnormal in autism. The recent identification of a de novo *EPHB2* kinase domain mutation in an individual with autism suggests that a deficit in EphB forward signaling might result in abnormal brain wiring and enhanced risk for autism.

Author contributions: M.A.R., M.E.G., M.H., and C.W.C. designed research; M.A.R., G.C., H.-Y.H.H., and K.Y.K. performed research; M.A.R., G.C., H.-Y.H.H., M.J.S., C.D., N.Š., M.E.G., and M.H. contributed new reagents/analytic tools; M.A.R., G.C., H.-Y.H.H., N.Š., M.E.G., M.H., and C.W.C. analyzed data; and M.A.R. and C.W.C. wrote the paper.

The authors declare no conflict of interest.

[1]To whom correspondence may be addressed. E-mail: cwcowan@mclean.harvard.edu or meg@hms.harvard.edu.

[2]M.H. and C.W.C. contributed equally to this work.

This article contains supporting information online at www.pnas.org/lookup/suppl/doi:10.1073/pnas.1324215111/-/DCSupplemental.

EphB2$^{-/-}$) mice at postnatal day 0 (P0). In *EphB1*$^{-/-}$ mice, we observed significant axon guidance defects within the VTel and adjacent to the IC—guidance errors that were not observed in either WT or *EphB2*$^{-/-}$ mouse brains (Fig. 1 *A*–*C*). Specifically, *EphB1*-deficient mice showed disorganization of the radial array of cortical and thalamic axons spanning between the cortical IZ and the IC (Fig. 1 *D* and *E*), and we observed large axon bundles that aberrantly extended toward the ventral brain floor (Fig. 1 *D* and *E* and Fig. S1). Interestingly, *EphB1/2 DKO* mutant mice had a more severe guidance defect compared with *EphB1*$^{-/-}$ mice (Fig. 2 *A* and *G* and Figs. S1 and S2), indicating that EphB2 can partially compensate for the loss of EphB1.

EphB Receptor Forward Signaling Mediates Proper Axon Guidance in the VTel. To test whether EphB forward signaling is required, we analyzed truncated EphB knockin (KI) mutant mice (*EphB1*$^{Tr/Tr}$ or *EphB2*$^{Tr/Tr}$) in which their intracellular domains are replaced with β-galactosidase (*lacZ*) (23, 24). These chimeric EphB receptors are expressed at the cell surface and mediate ephrinB-mediated reverse signaling in vivo, but lack EphB forward signaling events. *EphB1*$^{Tr/Tr}$ mice had similar axon guidance errors in the VTel as *EphB1*$^{-/-}$ mice, including a similar phenotypic severity and penetrance (Fig. 2 *B* and *G*), whereas mice lacking EphB2 forward signaling (*EphB2*$^{Tr/Tr}$) had normal VTel axon patterning (Fig. *C* and *G*). *EphB1*$^{Tr/Tr}$*EphB2*$^{Tr/Tr}$ double KI mice displayed a more severe, hyperfasciculated VTel misprojection phenotype (Fig. 2 *D* and *G*), similar to the VTel guidance errors observed in *EphB1/2 DKO* mice.

We next analyzed an analog-sensitive EphB receptor KI mouse (*AS-EphB*) that possesses point mutations within the conserved intracellular kinase domain that renders the endogenous

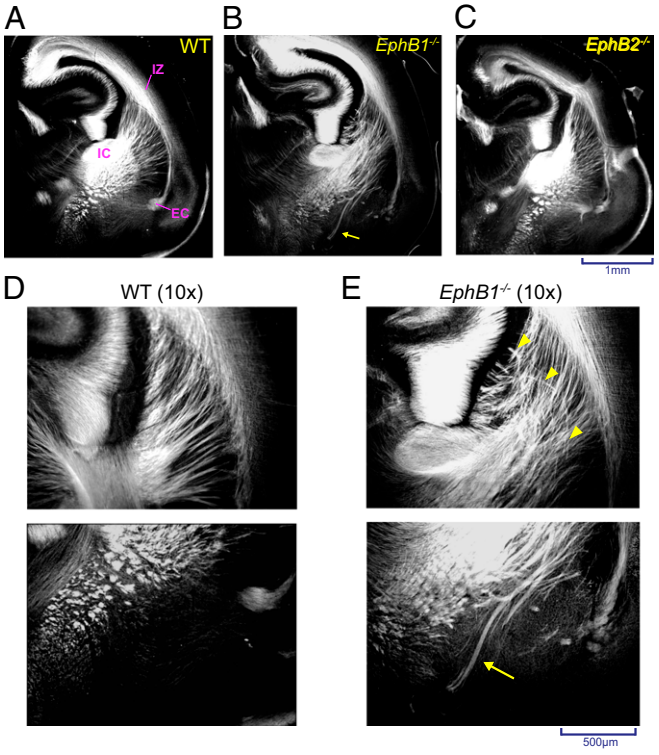

Fig. 1. VTel axon guidance errors in *EphB1*$^{-/-}$ mice. Representative coronal sections (approximate distance of coronal sections to bregma = 3.7 mm) of L1-CAM immunostained (*A*) WT, (*B*) *EphB1*$^{-/-}$, or (*C*) *EphB2*$^{-/-}$ mouse brains at P0. (*B* and *E*) L1-CAM^{+} axons in the ventral-most VTel. (*D* and *E*) Magnified image (10×) showing disorganized axons within the dorsal striatal region (yellow arrow heads in *E*, *Upper*) and misrouted fibers in the ventral VTel (yellow arrow in *E*, *Lower*). EC, external capsule.

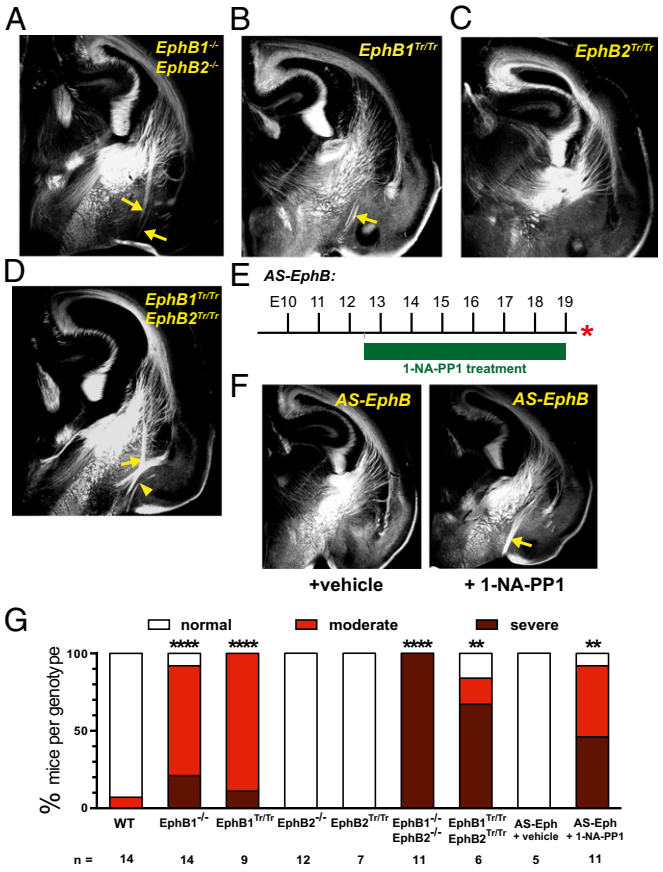

Fig. 2. EphB forward signaling is required for normal axon guidance in the VTel. L1-CAM–immunolabeled coronal sections of (*A*) *EphB1*$^{-/-}$*EphB2*$^{-/-}$, (*B*) *EphB1*$^{Tr/Tr}$, (*C*) *EphB2*$^{Tr/Tr}$, or (*D*) *EphB1*$^{Tr/Tr}$*EphB2*$^{Tr/Tr}$ mutant mice at P0. The axon guidance errors in the VTel are noted with yellow arrows. In the *EphB1*$^{Tr/Tr}$*EphB2*$^{Tr/Tr}$ mice, evidence of a misprojected posterior branch of the anterior commissure is noted by yellow arrowhead. (*E* and *F*) Injection of the EphB kinase inhibitor, 1-NA-PP1, from E12–E19 produced VTel axon guidance errors. (*G*) Quantification of VTel axon guidance errors, as described in *SI Methods*. $^{**}P < 0.01$, $^{****}P < 0.0001$, Fisher's exact test (Fig. S2).

EphB1–3 receptors sensitive to the reversible kinase inhibitor, 1-NA-PP1, in vivo (25). Twice daily injections of vehicle or 1-NA-PP1 (80 mg/kg) to timed-pregnant *AS-EphB* mutant (or WT control) mice from E12.5 to E19.0 resulted in significant VTel axon guidance errors, including severe ventral misprojections (Fig. 2 *E*–*G* and Figs. S2 and S3; see Fig. S6*B*). The severity of the inhibitor-injected *AS-EphB* mutant phenotype was reduced in drug-injected *AS-EphB* mutants compared with EphB truncated mutant mice, possibly due to partial effects of kinase-independent roles for the EphB intracellular domain or incomplete inhibition of the mutant EphB receptor kinase activity in vivo. Nonetheless, these findings specifically implicate EphB tyrosine kinase activity in VTel axon guidance in vivo.

EphB1/2 Receptors Mediate Thalamic Axon Guidance in the VTel. We next analyzed control and *EphB1/2 DKO* mutant mice at earlier developmental periods when most thalamic and cortical axons are first navigating within the VTel (e.g., E12.0–14.5). At E14.5, ascending L1-CAM^{+} TCAs populate the ventral-most portions of the VTel and have already reached the IZ beneath the cortical plate (26), whereas descending deep-layer cortical axons have only penetrated the dorsal half of the VTel (4, 27) (Fig. 3*A* and Fig. S4). To selectively visualize axons derived from cortical subplate and deep-layers regions, we used: (*i*) *FezF2*-GFP mice that express GFP in both deep layer and subplate cortical neurons

DEVELOPMENTAL BIOLOGY

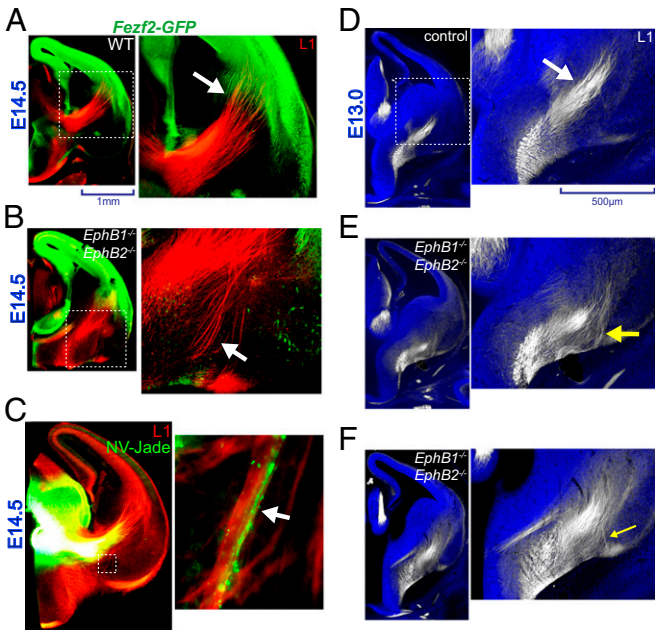

Fig. 3. TCAs in VTel are misguided in EphB-deficient mice. (*A* and *B*) Coronal sections of E14.5 *Fezf2-GFP* brains double-labeled for GFP (green, cortical axons) and L1-CAM (red, thalamic axons). At this stage, most GFP$^+$ cortical pioneer axons have penetrated the dorsal-most portion of the VTel (white arrow in *Inset*), whereas L1-CAM$^+$ TCAs have extended through the VTel into the cortical IZ. (*B*) Coronal section of a *Fezf2-GFP;EphB1/2 DKO* mouse brain with L1-CAM$^+$ axon guidance errors in VTel (white arrow in *Inset*). (*C*) NV-Jade fluorescent anterograde tracer (green) placed in the thalamus of E14.5 *EphB1/2 DKO* brain. The labeled thalamic axons colabel with misprojected L1-CAM$^+$ axons in the VTel of *EphB1/2 DKO* mice at E14.5. (*D*) Coronal section of an E13.0 littermate control embryo (*EphB1*$^{+/-}$*EphB2*$^{-/-}$) with L1-CAM labeling of ascending TCAs in the VTel (white arrow in *Inset*). Brain sections were counterstained with Hoechst nuclear stain (blue). (*E* and *F*) *EphB1/2 DKO* mice extend L1-CAM$^+$ axons into more ventral-lateral regions (yellow arrows in *Insets*) compared with control mice.

during development and in layer-5 cortical neurons specifically at postnatal ages (CFAs) (Fig. 3*A* and Fig. S4) (28), and (*ii*) *Golli*-tau-GFP mice that express a tau-GFP fusion protein under the control of the *Golli* gene promoter, which confers selective expression in cortical subplate and layer-6 neurons (CTAs) (Fig. S4) (27). In *Fezf2-GFP;EphB1/2 DKO* mice at E14.5, we observed clear L1-CAM$^+$ TCA guidance defects in the ventral VTel in a region ventral to the GFP$^+$ cortical axons (Fig. 3*B*). Thalamic anterograde axon labeling with a lipophilic fluorescent tracer revealed clear overlap with the misprojected VTel L1-CAM$^+$ axons (Fig. 3*C*).

Analysis of *EphB1/2 DKO* mice at E13.0—a time when thalamic axons are selectively labeled by L1-CAM antibodies in the ventral VTel (26, 29) and when the TCAs are turning dorsally across the DTB *en route* to the cortical plate (reviewed in refs. 9 and 15) —we observed a subpopulation of L1-CAM$^+$ axons that projected laterally in the ventral VTel (Fig. 3 *D* and *F*). Some of these mislocalized fibers showed a delayed dorsal turn into the dorsal VTel (Fig. 3 *E* and *F*, arrows).

To determine when and where EphB1 and EphB2 are expressed during the periods when the TCA guidance errors were first being observed (~E13), we analyzed β-gal expression in *EphB1*$^{Tr/+}$ or *EphB2*$^{Tr/+}$ mice using X-gal staining for the EphB1–lacZ or EphB2–lacZ fusion protein (23, 24). We observed strong expression of EphB1–lacZ in a restricted region of the caudal thalamus (Fig. 4*A*, arrow) and within the VTel region, whereas EphB1 was largely undetectable in cortical plate regions at E13 (Fig. 4*A*). EphB2–*lacZ* expression was also observed in the caudal thalamus at E13.0 (Fig. S5), albeit in a distinct, but overlapping, pattern compared with EphB1. Because EphB1 and EphB2 are most highly expressed in the caudal thalamus, we labeled the rostral and caudal thalamus with two different anterograde lipophilic dyes to study the topography of TCA fibers within the ventral VTel. In control mice, caudal TCAs populated the ventral–lateral region of ascending VTel axons, whereas the rostral TCAs populate the dorsal–medial portion of the ascending TCA fibers in the VTel (Fig. 4*B*), suggesting that caudal thalamic axons navigate selectively in the ventrolateral-most regions of the VTel. Using this approach in *EphB1/2 DKOs* at E14.5, misprojected VTel axons were exclusively labeled with the caudal, but not rostral, thalamic dyes, suggesting misprojected axons in *EphB1/2 DKO* mice are largely derived from caudal thalamus (Fig. 4*C*, arrow).

Deep-Layer Cortical Axon Guidance Errors in EphB Mutant Mice. During normal development, CFA (layer 5) and CTA (layer 6) fiber projections navigate together through the VTel and into the IC (2, 30), and are thought to cofasciculate or comingle with ascending thalamic fibers. In the *EphB1/2 DKO* mice at P0, we observed that the misguided VTel axon fascicles (L1-CAM$^+$) colabeled with both CFA and CTA axons (Fig. 5 *A* and *B*), indicating that a subpopulation of CTAs and CFAs misproject into the same VTel region as, and possibly via cofasciculation with,

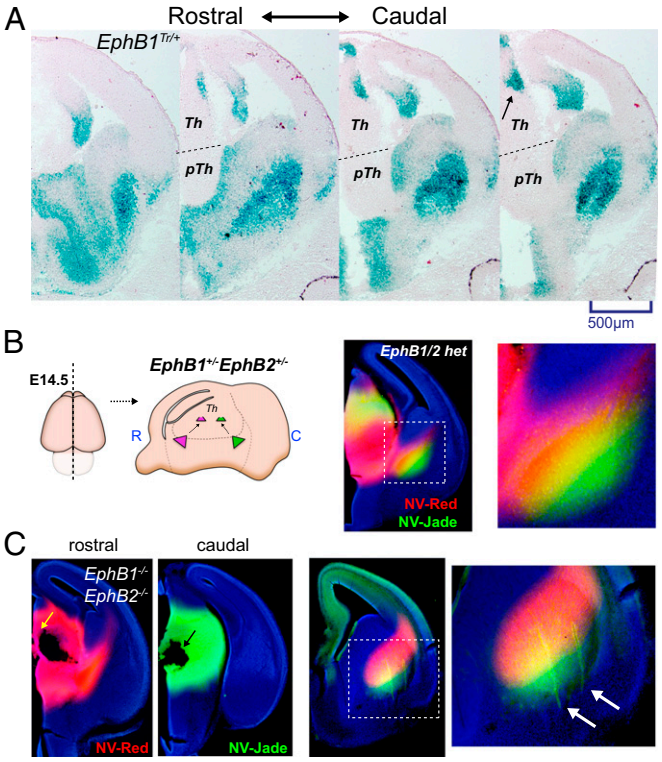

Fig. 4. Caudal thalamic axons populate the ventrolateral portion of the VTel TCA. (*A*) X-gal staining of coronal sections for E13.0 *EphB1*$^{Tr/+}$ mice show a low-rostral to high-caudal thalamic expression of EphB1-lacZ (arrow). LacZ expression is also observed throughout the VTel region and in the hippocampal region, but is largely absent in cortical regions. (*B*) Diagram of the dual thalamic labeling at E14.5 using NeuroVue-Red (NV-Red) tracer (rostral thalamus) and NeuroVue-Jade (NV-Jade) tracer (caudal). In control mice (*EphB1*$^{+/-}$*EphB2*$^{+/-}$), the caudal thalamic placements preferentially labeled the ventrolateral TCA populations in the VTel, whereas the rostral thalamic placements (red) labeled the dorsomedial TCA populations (see *Inset*). (*C*) Same as in *B*, except labeling of *EphB1/2 DKO* mice at E14.5. Rostral and caudal tracer placements are shown (yellow and black arrow, respectively). Caudal thalamic tracers selectively labeled misprojected TCAs in VTel (green; white arrows in *Inset*) of *EphB1/2 DKO* embryos.

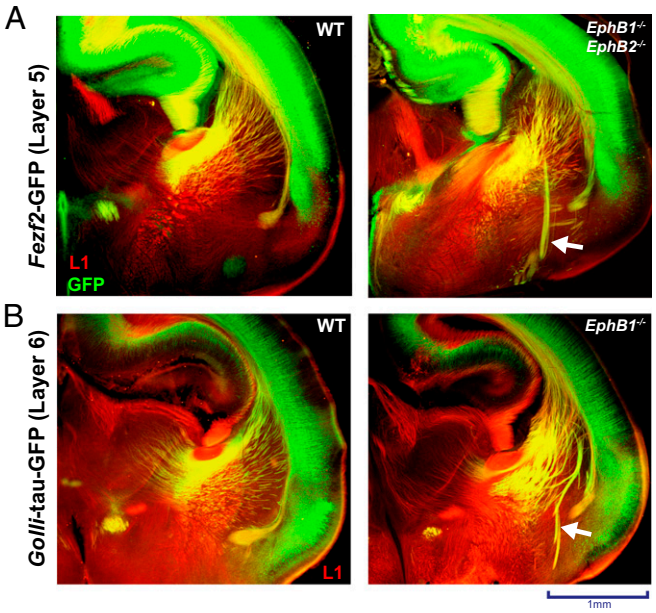

Fig. 5. Deep-layer cortical axons are misguided in the VTel of EphB-deficient mice. Immunostaining of L1-CAM (red) and GFP (green) in P0 brains (coronal; approximate distance of coronal sections to bregma = 3.7 mm) show axon guidance errors contain cortical axons. (*A*) *Fezf2-GFP* transgenic mice [WT (*Left*) or *EphB1*$^{-/-}$*EphB2*$^{-/-}$ (*Right*)] reveal that cortical layer-5 axons (green) are mistargeted in the VTel region (white arrow). (*B*) *Golli-tau-GFP* transgenic mice (WT or *EphB1*$^{-/-}$) reveal that cortical layer-6 axons (green) are mistargeted in the VTel region (white arrow) and colocalize with L1-CAM.

the earlier misprojected thalamic axons. Analysis of *Fezf2-GFP; EphB1/2 DKO* mice at E16.0, a developmental stage when most GFP^{+} cortical axons have descended midway through the VTel, revealed descending CFAs that were extending along, and highly intermingled with, the aberrant L1-CAM^{+} axon fascicles (Fig. 6*A*), suggesting that some cortical axons extend along preexisting, misprojected TCAs. Consistent with this observation, transient inhibition of EphB kinase activity in pregnant *AS-EphB* KI mice from E12.0 to E14.5, a time frame that spans early TCA guidance through the VTel, produced robust VTel axon guidance errors when analyzed at E19.5 (Fig. 6*B* and Fig. S6 *A* and *B*).

Analysis of Cortical Axon Guidance Errors in EphB Mutant Mice. To determine the origin of the misprojected cortical axons in EphB1/2 DKO mice, we placed NeuroVue carbocyanine dye-soaked filters into random positions across the entire cerebral cortex in *EphB1/2 DKO* (or control) mouse brains (P0), and analyzed anterograde-labeled cortical axons (Fig. 6*C*). With this approach, we efficiently labeled a limited number of descending cortical axons for each implanted brain (Fig. 6*D* and Fig. S6*C*), and observed that misprojected VTel axons originated from two discrete cortical subregions (Fig. 6*E*, red boxes). The largest cortical subregion mapped to the putative somatosensory cortex of the P0 brain, whereas the smaller cortical subregion localized to a border region of the putative somatosensory and auditory cortices. As such, these findings suggest that the misprojected cortical axons do not randomly misproject along TCA fascicles, but originate from discreet cortical subregions.

EphrinB1 Is Required for the TCA Guidance in the VTel. To determine the potential in vivo ligand for EphB1/2-dependent TCA guidance, we first assessed a likely candidate, *ephrinB2*, which is expressed in the ventral–lateral VTel at E13.0 (Fig. S7). Because *ephrinB2*$^{-/-}$ mice die prenatally at ages E9–E10 due to cardiac valve formation defects (31), we generated *ephrinB2* conditional KO (cKO) mice (32) by crossing floxed *ephrinB2* mice with *Nestin*^{Cre}, which generated cortical plate-specific recombination by E13.5, or *FoxG1*^{Cre}, which generated brain-wide recombination by E13.5 (Fig. S7). Neither of these *ephrinB2 cKO* mice had apparent VTel axon guidance defects, suggesting that *ephrinB2* is dispensable for TCA guidance.

We next analyzed ephrinB1 expression levels at E12.5–E14.5 using a Tet-inducible *ephrinB1*^{rtTA}*;TetO-tdTomato* reporter mouse line. At E12.5 and E13.5, we observed high levels of ephrinB1 expression in ventral–lateral VTel regions, dorsal VTel regions, and throughout the cortical plate, but no detectable expression in the thalamus (Fig. 7*A*). Interestingly, at E13.5 we also observed a region of ephrinB1 expression along the ventral brain border where TCA fibers are misguided in EphB-deficient conditions (Fig. 7*A*, yellow arrow), as well as the near complete absence of ephrinB1 in the TCA axon-spanning region of the ventral VTel (Fig. 7*A*, white arrow). To test whether *ephrinB1* is required for TCA guidance in the VTel, we generated brain-wide *ephrinB1* cKO mice (*FoxG1*$^{Cre/+}$*;ephrinB1*$^{loxP/Y}$). We observed significant TCA guidance errors at E13.0 reminiscent of the *EphB1/2 DKO* mice TCA errors (Fig. 7*B*). This strongly

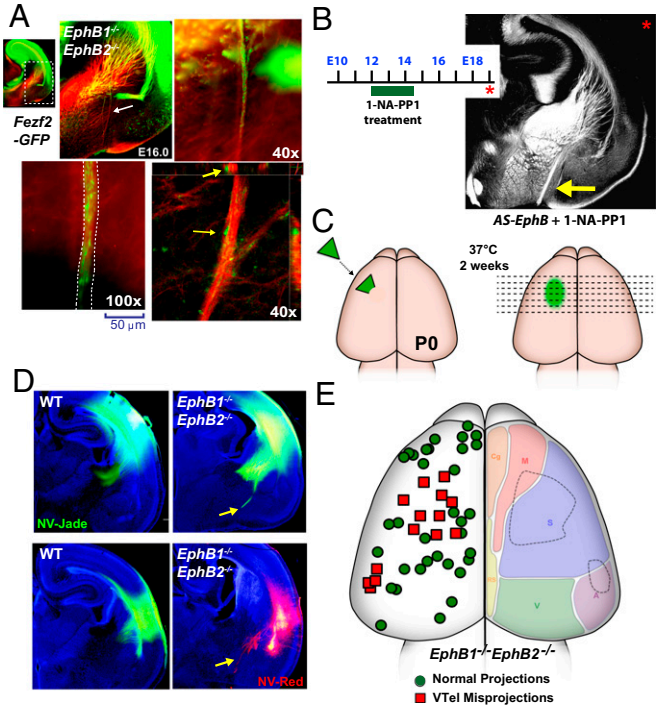

Fig. 6. Descending cortical axon misprojections originate from two specific neocortical subregions. (*A*) Coronal section of a *Fezf2-GFP;EphB1*$^{-/-}$*EphB2*$^{-/-}$ brain at E16.0 where VTel axon misprojections are evident (white arrow). Partial progression of misprojected GFP^{+} (green) axons along L1-CAM^{+} (red) axon fascicles suggests direct cofasciculation of the GFP^{+} axons with earlier misprojected thalamic fibers (yellow arrows). (*B*) Twice-daily 1-NA-PP1 injections (from E12 to E14.5) in timed-pregnant *AS-EphB* mutant dams produced L1-CAM^{+} VTel axon guidance errors (yellow arrow) when analyzed at E19. See quantification in Fig. S6*A*. (*C*) Diagram of the cortical subregion anterograde axon tracing analysis in P0 brains. (*D*) Example P0 coronal brain sections of WT or *EphB1/2 DKO* mice labeled with NV-Jade (green) or NV-Red (red) and Hoechst nuclear counterstain (blue). VTel axon misprojections were visualized in the *EphB1/2 DKO* brains (yellow arrows). (*E*) Map of axon tracer locations and VTel axon guidance errors from 48 separate *EphB1/2 DKO* mice brains reveals that most misguided axons derive from two discreet cortical subregions (dashed lines, right hemisphere). The anterograde tracer placements were mapped and designated as containing some VTel axon guidance errors (red square) or containing no VTel axon guidance errors (green circles). The right hemisphere diagrams the approximate location of functional subregions of a WT, P0 mouse cortex. A, auditory; Cg, cingulate; M, motor; RS, retrospenial; S, somatosensory; V, visual.

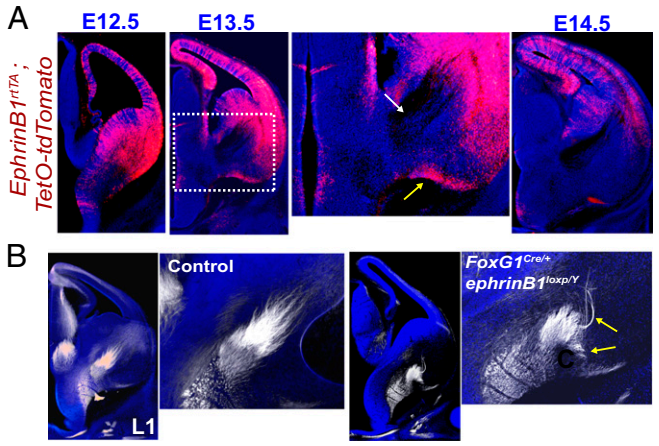

Fig. 7. VTel axon guidance errors in *EphrinB1* cKO mice. (*A*) Coronal brain sections of *ephrinB1-rtTA;TetO-tdTomato* reporter embryos from ages E12.5, E13.5 and E14.5 (each $n = 2$). EphrinB1 expression, reported by tdTomato (red), is high in the VTel at E12- E13.5, but is dramatically decreased in the VTel by E14.5. At E13.5, ephrinB1 (tdTomato) is expressed around the VTel region where ascending thalamic axons are located (white arrow in *Inset*). A strong region of ephrinB1 expression forms the boundary along the ventral floor of the brain (yellow arrow in *Inset*). (*B*) E13.0 coronal sections of littermate control (FoxG1^{Cre+};*ephrinB1*$^{loxP/+}$) and *ephrinB1* cKO (FoxG1^{Cre+}; *ephrinB1*$^{loxP/y}$) brains immunolabeled with anti–L1-CAM (white) and nuclear stain (blue). Images to the right depict higher magnification insets of the VTel for control and cKO brains. L1-CAM^{+} thalamic axons are misprojected in ephrinB1 cKO mice (yellow arrows). See quantification in Fig. S7*G*.

suggests that ephrinB1 is a critical ligand for EphB1/2 in normal TCA guidance.

Discussion

We report here that EphB1, and to a lesser extent EphB2, kinase-dependent signaling plays an essential role in the proper guidance of TCAs in the VTel region of the developing mammalian forebrain in vivo. EphB1 and EphB2 receptors are expressed in the developing caudal thalamus at a time when TCAs are turning from the ventral–portion of the VTel toward the IZ and developing cortical plate. In addition, ephrinB1 is expressed in regions surrounding the developing TCA fibers in the VTel, and *ephrinB1* cKO mice have TCA guidance errors similar to *EphB1/2 DKO* mice. Finally, we find that in *EphB1/2 DKO* mice descending cortical axons from discrete cortical subregions are misprojected in the VTel. As such, our data suggest that, at least in some cases, specific TCAs might selectively cofasciculate with descending cortical axons from discrete functional subregions to facilitate proper reciprocal connectivity (Fig. S8), generally consistent with the handshake model of cortical–thalamic reciprocal connectivity.

The major contributor to our observed cortical–thalamic axon guidance phenotypes, EphB1, is highly expressed in the caudal thalamus during TCA navigation in the VTel (Fig. 4*A*). Interestingly, this caudal thalamic region preferentially populates the most ventral–lateral portion of the ascending TCA axons (Fig. 4*B*) and is adjacent to the ventral–lateral VTel region of ephrinB1 expression (Fig. 7*A*). Based on the expression patterns of EphB1, EphB2, and ephrinB1 and the timing and location of axon guidance errors in the VTel, our findings suggest that EphB1/2 receptors in caudal thalamic neurons mediate repulsive axon guidance when they encounter ephrinB1 expressed in the ventrolateral VTel (Fig. S8). However, because EphB1 expression is found in both thalamus and VTel regions, future analysis of *EphB1* cKO mice with thalamic-, cortical- or VTel-selective gene deletion will better address the questions of whether (*i*) EphB1 in thalamic neurons functions cell autonomously to mediate normal TCA guidance in the VTel (*ii*), EphB1 functions in cells of the VTel region to control normal axon guidance, and/or (*iii*) whether cortical EphB1 receptors play a critical role in the guidance of deep-layer cortical axons and their thalamic axon counterparts.

Previous studies have described the guidance mechanisms that properly guide TCA fibers along their lateral and longitudinal pathways to the developing neocortex (reviewed in ref. 9). Multiple axon guidance ligands and receptors regulate TCA development (5, 6, 8, 33–35). EphrinA5 is expressed within the VTel along a high-rostral to low-caudal gradient that maintains proper topographic organization of EphA-expressing TCAs from the rostro–medial thalamus to their rostral–cortical target regions (5). In addition, migration of *Nkx2.1*-expressing cells within the developing VTel has been proposed to organize a TCA permissive corridor by creating a ventral repulsive boundary (36–38). Unexpectedly, in WT mice at E13, we observed that the vast majority of the thalamic-derived L1-CAM^{+} axons (26, 29) did not avoid the Nkx2.1-expressing region, but rather overlapped this population almost completely (Fig. S9). Our findings suggest that the Nkx2.1^{+} region is largely permissive to L1-CAM^{+} TCAs at E13.0, but switches to a repulsive region later in embryonic development and pushes TCA fibers into a more structured, dorsal–medial VTel region to form the mature IC.

The handshake hypothesis, first proposed more than 20 y ago, was based on the observation that deep-layer cortical axons and TCAs closely interact or comingle. As such, it was proposed that the handshake between these reciprocal fibers might be critical for guiding these axons to their target synaptic zones (13–15), although evidence against this model also exists (37, 39). Although our current study does not directly test the handshake hypothesis, our findings do support the general idea, and further extend its implications for coding reciprocal connectivity. Our findings suggest that EphB1/2 and ephrinB1 assist in the proper navigation of caudal thalamic axons within the VTel, and it is tempting to speculate that this TCA subpopulation might express unique cell surface proteins (e.g., cell adhesion molecules) that selectively cofasciculates with descending cortical axons from discreet cortical subregions to facilitate reciprocal, functional cortical–thalamic connectivity.

Several studies report developmental abnormalities in white matter tracts in autism spectrum disorder individuals (40–42), suggesting that deficits in normal axon guidance and connectivity might contribute to the pathophysiology of autism. The recent association of a de novo nonsense mutation in the *EPHB2* kinase domain to autism (43) suggests that a deficit in EphB forward signaling increases risk for autism.

Taken together, our findings describe a critical role for EphB1 and EphB2 receptor forward signaling in the process of TCA guidance. Moreover, our findings suggest that selective interactions between caudal-derived, ascending TCAs and descending deep-layer cortical axons might contribute to proper reciprocal connectivity in early development via selective cofasciculation.

Methods

Animals. All *EphB* mutant mice were previously described (23–25, 44). *EphrinB1*^{loxp} and *EphrinB2*^{loxp} cKO mice were previously described (32, 45). *Nestin*^{Cre} mice were provided by A. Eisch (The University of Texas Southwestern Medical Center), and *FoxG1*^{Cre} mice were acquired from Jackson Laboratories (46). *EphrinB2*^{Tr} mice (previously notated as *EphrinB2*^{lacZ}) express a truncated ephrinB2 protein fused to β-gal (47). *Rosa-tdTomato* and *TetO-tdTomato* mice were acquired from Jackson Laboratories (48, 49). The *Fezf2-GFP* and *Golli-tau-GFP* transgenic mice are previously described (27, 28). PCR genotyping was performed using published primer sets. All animal procedures were performed in accordance with approved Institutional Animal Care and Use Committee (IACUC) guidelines of the University of Texas Southwestern Medical Center, McLean Hospital, and Harvard Medical School.

Tissue Processing. For E12.5–E14.5 embryos, heads were removed and immediately postfixed in 3.7% (vol/vol) formaldehyde. For E15.5– P0, the brains were dissected away from the skull before postfixation in 3.7% (vol/vol) formaldehyde or a 4% (wt/vol) paraformaldehyde/2% (wt/vol) sucrose solution.

All postfixed tissue was fixed at 4 °C for 48 h before rinsing with PBS and storage at 4 °C in PBS + 0.02% Na-Azide. β-Gal staining of brain slices was previously described (23, 24). Immunostaining of free floating brain sections was performed on 70-μm coronal sections cut (vibratome) from brains embedded in a 1.5% (wt/vol) mix of 0.75% Low-Melting Point Agarose (Promega) and 0.75% standard Agarose (Fisher). Sections were immersed in blocking solution [5% (vol/vol) normal donkey serum, 1% BSA, 0.2% glycine, 0.2% lysine with 0.3% TritonX-100 in PBS] and incubated for 1 h at room temperature. Carbocyanine dye-labeled sections (see Axon Tracing) were blocked with the same solution except with 0.01% Triton X-100. Sections were next incubated overnight at 4 °C with either rat anti–L1-CAM, 1:200 (Millipore; MAB5272MI), rabbit anti-GFP, 1:2,000 (Life Tech; A11122), and/or rabbit anti-TTF1 (anti–Nkx2-1), 1:200 (Abcam; 20441) diluted in blocking solution, before incubation with either Cy3-conjugated donkey anti-rat IgG (Jackson Laboratories) and/or Alexa488-conjugated goat anti-rabbit IgG (Life Tech), and all sections were counterstained with 50 μg/mL Hoechst 33342 (Life Tech; H21492).

Axon Tracing. Anterograde dye tracing of cortical axons and thalamic axons was performed using focal application of NeuroVue Jade or NeuroVue Red carbocyanine dye filters (MTTI) placed directly into either the neocortex of fixed P0 brains or the thalamus of fixed hemisected E14.5 brains. Dye-implanted P0 brains were incubated at 37 °C for 2 wk (E19–P0 brains) or 1 wk (E14.5 brains) before sectioning. Dye-labeled brains were embedded in 1.5% (wt/vol) agarose before coronal vibratome sectioning (70 μm). Sections were either serially mounted onto glass slides with Aquamount (Thermo Scientific) and counterstained with Hoechst 33342 (Life Tech; 50 μg/mL) or were subsequently immunolabeled for anti–L1-CAM (see Tissue Processing). Focal application points of the NeuroVue dye filter within the neocortex were mapped using a P0 mouse brain atlas (50).

ACKNOWLEDGMENTS. The authors wish to thank Yuhong Guo and Kevin Kelly for technical assistance. This project was supported in part by Simons Foundation Autism Research Initiative Grant 240332 (to C.W.C.); by National Institutes of Health Grants R01 EY018207 (to C.W.C.), R01 MH66332 (to M.H.), R01 NS045500 (to M.E.G.), and RO1 NS054273 (to N.Š.); and by National Institute on Drug Abuse Training Grant T32 DA07290 (to M.A.R.).

1. Chédotal A, Richards LJ (2010) Wiring the brain: The biology of neuronal guidance. *Cold Spring Harb Perspect Biol* 2(6):a001917.
2. O'Leary DD, Koester SE (1993) Development of projection neuron types, axon pathways, and patterned connections of the mammalian cortex. *Neuron* 10(6):991–1006.
3. Alitto HJ, Usrey WM (2003) Corticothalamic feedback and sensory processing. *Curr Opin Neurobiol* 13(4):440–445.
4. Auladell C, Pérez-Sust P, Supèr H, Soriano E (2000) The early development of thalamocortical and corticothalamic projections in the mouse. *Anat Embryol (Berl)* 201(3): 169–179.
5. Dufour A, et al. (2003) Area specificity and topography of thalamocortical projections are controlled by ephrin/Eph genes. *Neuron* 39(3):453–465.
6. López-Bendito G, et al. (2007) Robo1 and Robo2 cooperate to control the guidance of major axonal tracts in the mammalian forebrain. *J Neurosci* 27(13):3395–3407.
7. Torii M, Levitt P (2005) Dissociation of corticothalamic and thalamocortical axon targeting by an EphA7-mediated mechanism. *Neuron* 48(4):563–575.
8. Wright AG, et al. (2007) Close homolog of L1 and neuropilin 1 mediate guidance of thalamocortical axons at the ventral telencephalon. *J Neurosci* 27(50):13667–13679.
9. López-Bendito G, Molnár Z (2003) Thalamocortical development: How are we going to get there? *Nat Rev Neurosci* 4(4):276–289.
10. Kwan KY, Sestan N, Anton ES (2012) Transcriptional co-regulation of neuronal migration and laminar identity in the neocortex. *Development* 139(9):1535–1546.
11. Molnár Z, Adams R, Blakemore C (1998) Mechanisms underlying the early establishment of thalamocortical connections in the rat. *J Neurosci* 18(15):5723–5745.
12. Molnár Z, Adams R, Goffinet AM, Blakemore C (1998) The role of the first postmitotic cortical cells in the development of thalamocortical innervation in the reeler mouse. *J Neurosci* 18(15):5746–5765.
13. Blakemore C, Molnár Z (1990) Factors involved in the establishment of specific interconnections between thalamus and cerebral cortex. *Cold Spring Harb Symp Quant Biol* 55:491–504.
14. Molnár Z, Blakemore C (1995) How do thalamic axons find their way to the cortex? *Trends Neurosci* 18(9):389–397.
15. Molnár Z, Garel S, López-Bendito G, Maness P, Price DJ (2012) Mechanisms controlling the guidance of thalamocortical axons through the embryonic forebrain. *Eur J Neurosci* 35(10):1573–1585.
16. Egea J, Klein R (2007) Bidirectional Eph-ephrin signaling during axon guidance. *Trends Cell Biol* 17(5):230–238.
17. Pasquale EB (2005) Eph receptor signalling casts a wide net on cell behaviour. *Nat Rev Mol Cell Biol* 6(6):462–475.
18. Shen K, Cowan CW (2010) Guidance molecules in synapse formation and plasticity. *Cold Spring Harb Perspect Biol* 2(4):a001842.
19. Cowan CW, et al. (2005) Vav family GEFs link activated Ephs to endocytosis and axon guidance. *Neuron* 46(2):205–217.
20. Srivastava N, Robichaux MA, Chenaux G, Henkemeyer M, Cowan CW (2013) EphB2 receptor forward signaling controls cortical growth cone collapse via Nck and Pak. *Mol Cell Neurosci* 52:106–116.
21. Mendes SW, Henkemeyer M, Liebl DJ (2006) Multiple Eph receptors and B-class ephrins regulate midline crossing of corpus callosum fibers in the developing mouse forebrain. *J Neurosci* 26(3):882–892.
22. North HA, et al. (2009) Promotion of proliferation in the developing cerebral cortex by EphA4 forward signaling. *Development* 136(14):2467–2476.
23. Chenaux G, Henkemeyer M (2011) Forward signaling by EphB1/EphB2 interacting with ephrin-B ligands at the optic chiasm is required to form the ipsilateral projection. *Eur J Neurosci* 34(10):1620–1633.
24. Henkemeyer M, et al. (1996) Nuk controls pathfinding of commissural axons in the mammalian central nervous system. *Cell* 86(1):35–46.
25. Soskis MJ, et al. (2012) A chemical genetic approach reveals distinct EphB signaling mechanisms during brain development. *Nat Neurosci* 15(12):1645–1654.
26. Fukuda T, et al. (1997) Immunohistochemical localization of neurocan and L1 in the formation of thalamocortical pathway of developing rats. *J Comp Neurol* 382(2): 141–152.
27. Jacobs EC, et al. (2007) Visualization of corticofugal projections during early cortical development in a tau-GFP-transgenic mouse. *Eur J Neurosci* 25(1):17–30.
28. Kwan KY, et al. (2008) SOX5 postmitotically regulates migration, postmigratory differentiation, and projections of subplate and deep-layer neocortical neurons. *Proc Natl Acad Sci USA* 105(41):16021–16026.
29. Fushiki S, Schachner M (1986) Immunocytological localization of cell adhesion molecules L1 and N-CAM and the shared carbohydrate epitope L2 during development of the mouse neocortex. *Brain Res* 389(1-2):153–167.
30. Price DJ, et al. (2006) The development of cortical connections. *Eur J Neurosci* 23(4): 910–920.
31. Cowan CA, et al. (2004) Ephrin-B2 reverse signaling is required for axon pathfinding and cardiac valve formation but not early vascular development. *Dev Biol* 271(2): 263–271.
32. Gerety SS, Anderson DJ (2002) Cardiovascular ephrinB2 function is essential for embryonic angiogenesis. *Development* 129(6):1397–1410.
33. Bagri A, et al. (2002) Slit proteins prevent midline crossing and determine the dorsoventral position of major axonal pathways in the mammalian forebrain. *Neuron* 33(2):233–248.
34. Little GE, et al. (2009) Specificity and plasticity of thalamocortical connections in Sema6A mutant mice. *PLoS Biol* 7(4):e98.
35. Powell AW, Sassa T, Wu Y, Tessier-Lavigne M, Polleux F (2008) Topography of thalamic projections requires attractive and repulsive functions of Netrin-1 in the ventral telencephalon. *PLoS Biol* 6(5):e116.
36. Bielle F, et al. (2011) Emergent growth cone responses to combinations of Slit1 and Netrin 1 in thalamocortical axon topography. *Curr Biol* 21(20):1748–1755.
37. Deck M, et al. (2013) Pathfinding of corticothalamic axons relies on a rendezvous with thalamic projections. *Neuron* 77(3):472–484.
38. López-Bendito G, et al. (2006) Tangential neuronal migration controls axon guidance: A role for neuregulin-1 in thalamocortical axon navigation. *Cell* 125(1):127–142.
39. Bagnard D, Lohrum M, Uziel D, Püschel AW, Bolz J (1998) Semaphorins act as attractive and repulsive guidance signals during the development of cortical projections. *Development* 125(24):5043–5053.
40. Minshew NJ, Williams DL (2007) The new neurobiology of autism: Cortex, connectivity, and neuronal organization. *Arch Neurol* 64(7):945–950.
41. Mizuno A, Villalobos ME, Davies MM, Dahl BC, Müller RA (2006) Partially enhanced thalamocortical functional connectivity in autism. *Brain Res* 1104(1):160–174.
42. Wolff JJ, et al.; IBIS Network (2012) Differences in white matter fiber tract development present from 6 to 24 months in infants with autism. *Am J Psychiatry* 169(6):589–600.
43. Sanders SJ, et al. (2012) De novo mutations revealed by whole-exome sequencing are strongly associated with autism. *Nature* 485(7397):237–241.
44. Williams SE, et al. (2003) Ephrin-B2 and EphB1 mediate retinal axon divergence at the optic chiasm. *Neuron* 39(6):919–935.
45. Davy A, Aubin J, Soriano P (2004) Ephrin-B1 forward and reverse signaling are required during mouse development. *Genes Dev* 18(5):572–583.
46. Hébert JM, McConnell SK (2000) Targeting of cre to the Foxg1 (BF-1) locus mediates loxP recombination in the telencephalon and other developing head structures. *Dev Biol* 222(2):296–306.
47. Dravis C, et al. (2004) Bidirectional signaling mediated by ephrin-B2 and EphB2 controls urorectal development. *Dev Biol* 271(2):272–290.
48. Li L, et al. (2010) Visualizing the distribution of synapses from individual neurons in the mouse brain. *PLoS ONE* 5(7):e11503.
49. Madisen L, et al. (2010) A robust and high-throughput Cre reporting and characterization system for the whole mouse brain. *Nat Neurosci* 13(1):133–140.
50. Paxinos GH, Watson G, Koutcherov C, Wang YH (2007) *Atlas of the Developing Mouse Brain at E17.5, P0, and P6* (Elsevier, Amsterdam), 1st Ed.

Supporting Information

Robichaux et al. 10.1073/pnas.1324215111

SI Methods

Generation of BAC-Tg-ephrinB1-rtTA Mice. *BAC-Tg-ephrinB1-rtTA* (abb: *ephrinB1-rtTA*) mice contain the second-generation reverse tetracycline transactivator, *rtTA-2sM2*, knocked into the ORF of BAC *ephrinB1* sequences. Transgenic mice were generated as follows: BAC clone RP23-110A15, a BAC from a C57BL/6J background containing 27 kb upstream of the ephrin-B1 start codon, was purchased from the BACPAC resources center at the Children's Hospital Oakland (Oakland, CA). The cDNA for *rtTA-2sM2* was targeted into the *ephrin-B1* ORF in RP23-110A15 using bacterial homologous recombination (http://web.ncifcrf.gov/research/brb/recombineeringInformation.aspx). Briefly, RP23-110A15 was first transformed into EL250 strain cells, and then targeted with a modified pL451 vector containing an Frt-sandwiched Neo/Kan cassette and the cDNA for *rtTA-2sM2*, flanked by 500-bp homology arms (the targeting vector is thus *500bpLHA-rtTA-2sM2-Frt/Neo/Kan/Frt-500bpRHA*) guiding the cassette to the ORF of *ephrinB1*. Arabinose induction of *flpe* activity in the targeted BAC was then used to excise the Frt-Neo/Kan-Frt cassette, leaving *rtTA-2s-M2* followed by a single copy of *Frt* in the ephrinB1 ORF. Proper targeting of the *ephrinB1* ORF was confirmed by PCR and restriction endonuclease digests. Pronuclear injection of fertilized oocytes with this *BAC-Tg-ephrin-B1-rtTA* construct was performed by Transgenic Core facilities at the Department of Developmental Biology, The University of Texas Southwestern Medical Center. $EphrinB1^{rtTA}$ mutants were cross bred with *TetO-tdTomato* mice to yield the $ephrinB1^{rtTA}$;*TetO-tdTomato* reporter line. Doxycylcine (Dox) induction of *ephrinB1-rtTA*;*TetO-tdTomato* animals was performed systemically for ∼48 h by feeding animals Dox-treated chow (0.625 g/kg Dox hyclate, Harlan TD.08541) and including Dox in the drinking water (3 mg/mL).

Analysis of Axon Guidance Errors. L1-CAM– or GFP-immunolabeled brain sections, dye-labeled sections, and counterstained sections were imaged on an epifluorescent microscope. Photomicrograph images were produced using an Olympus DP70 CCD digital camera. Confocal *z*-stack images were obtained on a Zeiss LSM 510 Meta confocal microscope and *X-Y-Z* plane image analysis was performed with Volocity software (Perkin-Elmer). Pseudocoloring and adjustments in image brightness, contrast, and color balance were made for image clarity. Ventral telencephalon (VTel) axon guidance misprojection errors were scored, under experimenter-blinded conditions, as L1-CAM^{+} fibers that turned in a ventral fashion away from the internal capsule. The moderate misprojection phenotype was classified by the observation of a few thin axon bundles that became misprojected, whereas severe misprojection brains were classified by the presence of several misprojected fibers or thick misprojected fiber bundles.

1-NA-PP1 Administration. 1-NA-PP1 was synthesized as described previously (1, 2), and timed-pregnant wild-type (WT) or *AS-EphB* dam were injected s.c. twice daily with 80 mg/kg 1-NA-PP1 (dissolved in 10% DMSO, 20% Cremaphor-EL, 70% saline) before L1-CAM analysis at E19 (2).

Data Analysis. The Chi square analysis and Fisher's exact test were used to determine statistical significance in the axon misguidance phenotype scoring experiments. Statistics were compiled and graphs were designed using GraphPad Prism software.

1. Blethrow J, Zhang C, Shokat KM, Weiss EL (2004) Design and use of analog-sensitive protein kinases. *Curr Protoc Mol Biol* 66:18.11.1–18.11.19.

2. Soskis MJ, et al. (2012) A chemical genetic approach reveals distinct EphB signaling mechanisms during brain development. *Nat Neurosci* 15(12):1645–1654.

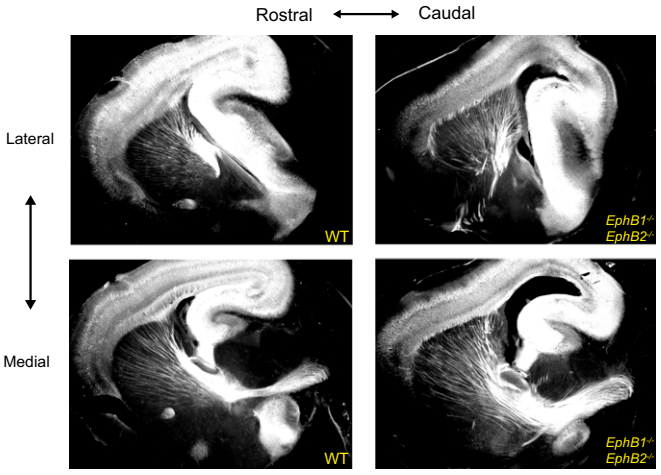

Fig. S1. Axon misprojections in EphB-deficient mice are localized in the lateral VTel. Sagittal vibratome sections of either P0 WT or $EphB1^{-/-}EphB2^{-/-}$ *DKO* mutant brains at a matching medial and lateral sagittal plane. Misprojected axons are largely present in the lateral *DKO* aspect. In addition, the rostral–caudal topography of axons in the VTel is maintained in *DKO* mutants.

A

	# brains with **no** misprojections	# brains with **any** misprojections	n-value
WT	13	1	14
EphB1$^{-/-}$	1	13	14
EphB1$^{Tr/Tr}$	0	9	9
EphB2$^{-/-}$	12	0	12
EphB2$^{Tr/Tr}$	7	0	7
EphB1$^{-/-}$EphB2$^{-/-}$	0	11	11
EphB1$^{Tr/Tr}$EphB2$^{Tr/Tr}$	1	5	6
AS-EphB Vehicle	5	0	5
AS-EphB Drug	1	10	11

**** p<0.0001 (Chi Square test)

B

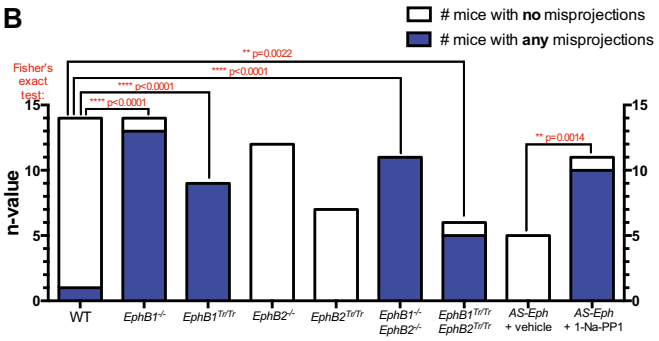

Fig. S2. EphB mutants have a statistically significant axon misprojection phenotype. (*A*) Contingency table of scored axon misprojection phenotypes outlined in Fig. 2*G* for Chi square statistical analysis. All mutant misprojection scores from Fig. 2*G* are combined in the second column. (*B*) Graphical representation of *A* with *P* values from Fisher's exact tests performed to directly compare various mutant genotypes.

A

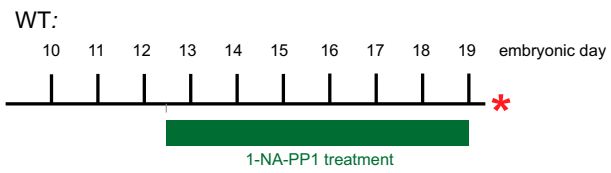

B

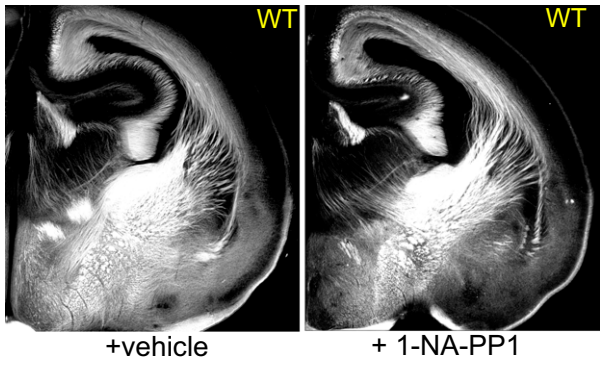

Fig. S3. WT embryos have normal VTel axon morphology upon 1-NA-PP1 drug adminstration. (*A*) Drug injection schedule for 1-NA-PP1 drug treatment of timed-pregnant WT mutants. These mice were administered twice-daily s.c. injections of 80 mg per kg of body weight 1-NA-PP1 or vehicle from E12.5 to E19.0. Embryos were collected for analysis at E19.5 (asterisk). (*B*) Representative L1-CAM–stained E19.5 coronal sections of WT embryos that were either administered 1-NA-PP1 or vehicle and immunostained with anti–L1-CAM. For both conditions, WT embryonic brains have normal L1-CAM^{+} VTel axon morphology (drug, $n = 6$; vehicle, $n = 4$).

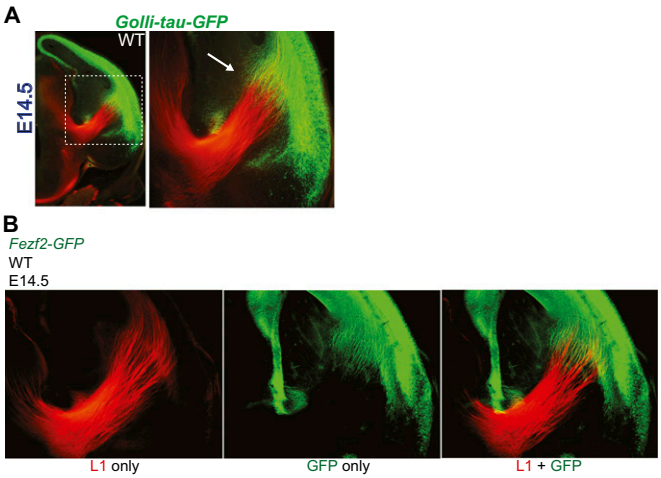

Fig. S4. L1-CAM$^+$ axons in the VTel are clearly derived from the thalamus at age E14.5. (*A*) E14.5 coronal brain section of a *Golli-tau-GFP* reporter embryonic mouse that is also WT for EphB expression, and which demonstrates the partial development of GFP$^+$ cortical pioneer axons in the early VTel (white arrow in *Inset*). (*B*) Coronal section of an E14.5 *Fezf2-GFP* embryonic brain that has WT EphB receptor expression and is immunostained with anti–L1-CAM (red), anti-GFP (green) and dual stain merged. L1-CAM$^+$ axons are clearly derived from the thalamus and ascend toward the cortical intermediate zone (IZ). GFP$^+$ cortical pioneer axons have only penetrated the dorsal half of the developing VTel at this early embryonic age (arrow in *A*), whereas L1-CAM$^+$ thalamocortical axons (TCAs) have developed extensively through the VTel toward the cortical IZ.

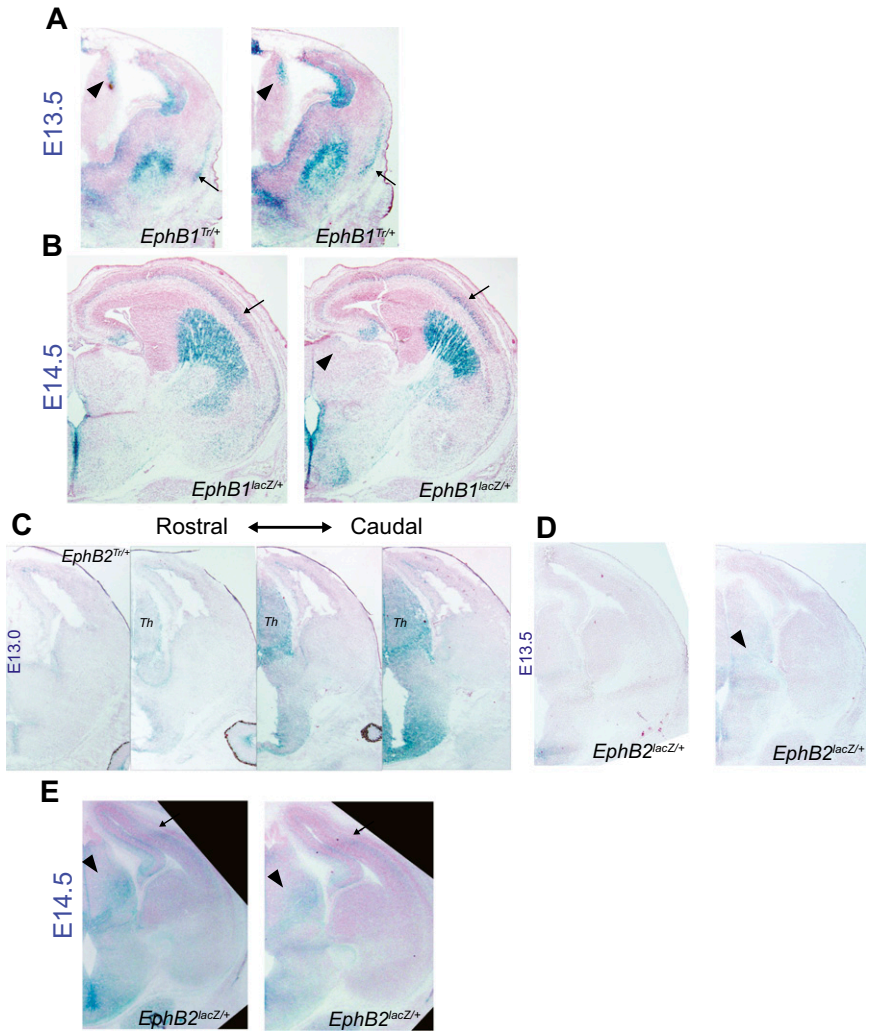

Fig. S5. EphB1 and EphB2 are not expressed in the cortical plate until age E14.5. Coronal brain sections of *EphB1*$^{Tr/+}$ truncated mutants at embryonic age (*A*) E13.5 and (*B*) E14.5 that are stained with X-gal to label β-galactosidase containing EphB1 truncated receptor protein. EphB1 protein expression is concentrated in the dorsal–caudal thalamus (Th) (arrowheads) and cortical plate (arrows). At E13.5, cortical EphB1 expression is exclusive the lateral cortical plate. (*C*) An E13.0 *EphB2*$^{Tr/+}$ mutant brain stained with X-gal. EphB2 expression is ubiquitously expressed throughout the caudal thalamus ($n = 3$). (*D*) E13.5 and (*E*) E14.5 *EphB2*$^{Tr/+}$(also annotated as *EphB2*$^{lacZ/+}$) mutant brains stained with X-gal. EphB2 expression continues throughout the caudal thalamus (arrowheads), and becomes expressed in the cortical plate at E14.5 (arrows).

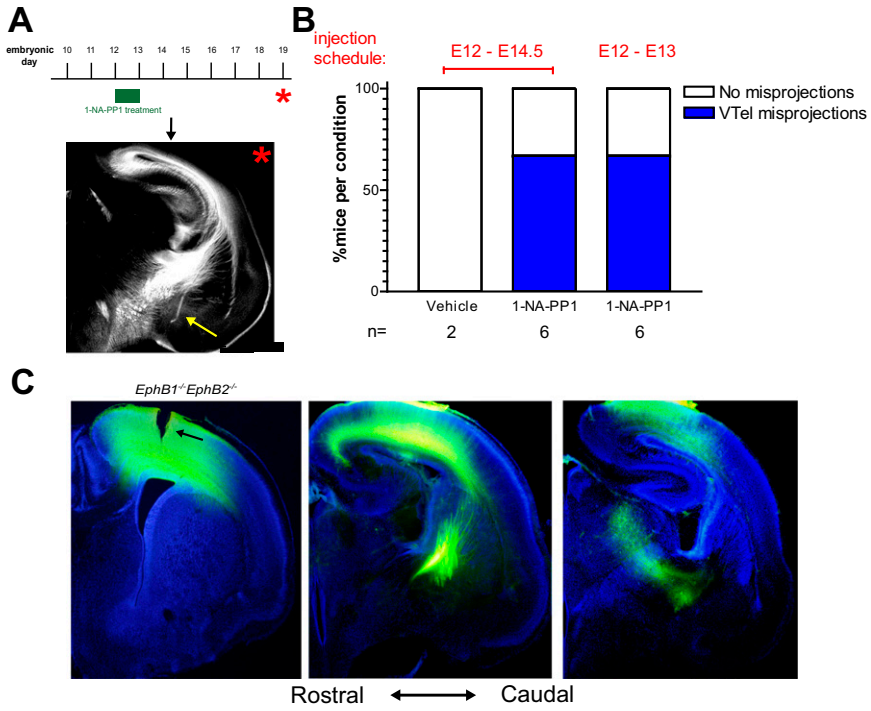

Fig. S6. Anterograde dye tracing from the neocortex labels the entire length of descending cortical axons. (*A*) Drug injection schedule for short-term 1-NA-PP1 drug treatment in timed-pregnant *AS-EphB* mutants. Twice-daily injections of 80 mg per kg of body weight drug were administered for the embryonic time points indicated (green box). Embryos were collected for analysis at E19.0 (asterisk) and fixed for immunoanalysis with anti–L1-CAM. Short-term injected (E12–13) *AS-EphB* mutant dams produced L1-CAM^{+} VTel axon guidance errors (yellow arrow) when analyzed at E19 (graph). (*B*) Graphical representation of VTel misprojections observed from short-term vehicle and 1-NA-PP1 exposure experiments outlined in Fig. 6*B*. (*C*) P0 coronal sections of an *EphB1/2 DKO* brain at postnatal day P0 that are labeled with NV-Jade tracer that is implanted into the dorsal neocortex (black arrow). Descending corticofugal axons from this neocortical origin point are labeled along their entire shaft length through the VTel, IC, and Th. Labeled axons from this example *DKO* brain do not become misprojected in VTel. Brain sections were counterstained with Hoechst nuclear stain (blue).

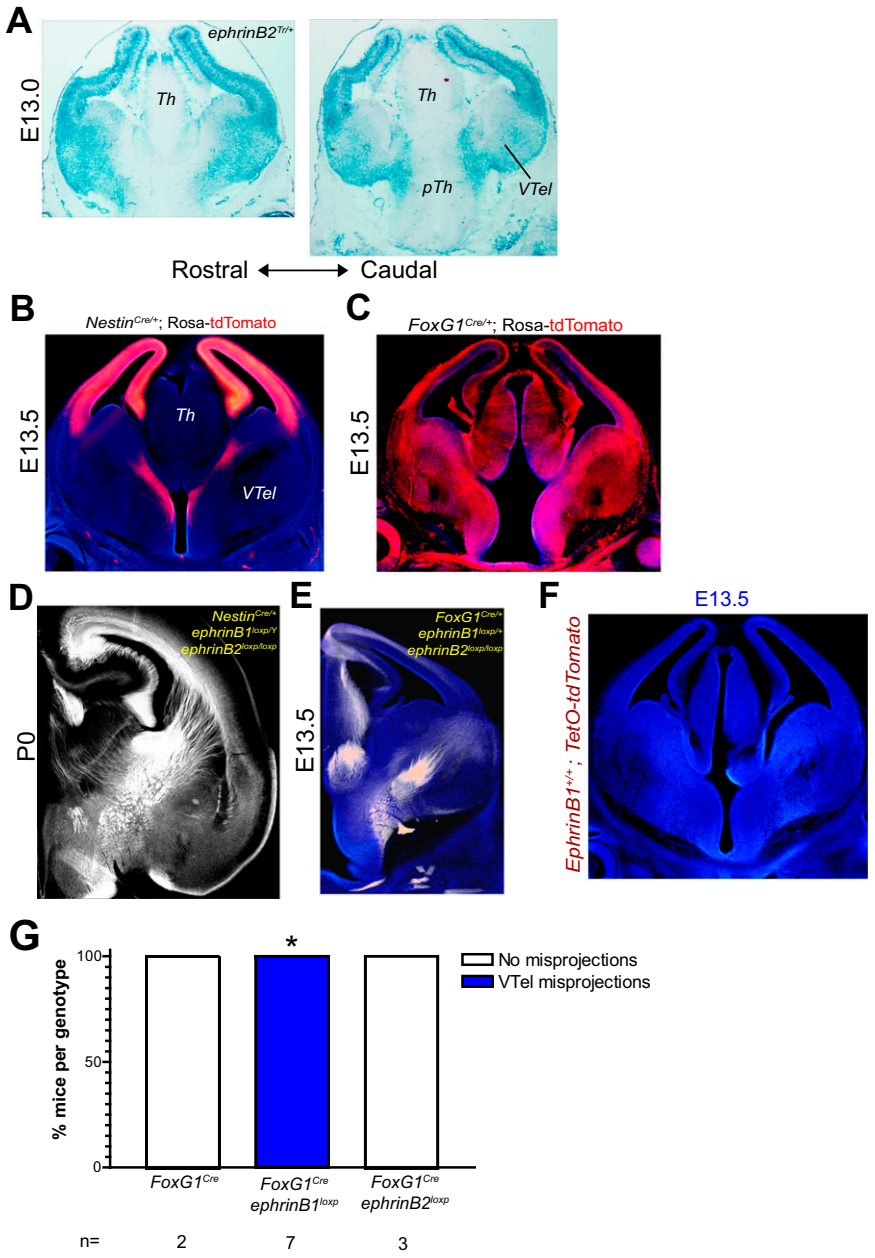

Fig. S7. EphrinB2 is not required for proper TCA guidance in the VTel. (*A*) Coronal brain sections of an *ephrinB2*$^{Tr/+}$ truncated mutant brain at embryonic age E13.0 stained with X-gal to label β-galactosidase containing ephrinB2 truncated receptor protein. At this age, ephrinB2 is highly expressed throughout the entire telencephalon including in the VTel where TCA axons are located; however, ephrinB2 is only lightly expressed in the thalamus (Th) and prethalamus (pTh) ($n = 3$). (*B*) Representative coronal section of an E13.5 embryonic brain containing the Nestin-Cre driver allele and *Rosa-tdTomato* reporter gene. Tomato signal (red) represents Nestin-Cre expression, which is specifically localized to the dorsal telencephalon including the developing cortical plate and hippocampal anlage, as well as migrating cells at the ventral midline. (*C*) Coronal section of a P0 *ephrinB1*$^{loxp/Y}$;*ephrinB2*$^{loxp/loxp}$ conditional mutant containing the Nestin-Cre driver allele. These conditional knockout (cKO) brains have normal axon wiring ($n = 6$), which indicates that the Nestin-Cre driven conditional deletion of ephrinB1/2 is not sufficient to phenocopy EphB receptor KO axon miswiring phenotypes. (*D*) Representative coronal section of an E13.5 embryonic brain containing the FoxG1-Cre driver allele and *Rosa-tdTomato* reporter gene. Unlike Nestin-Cre, FoxG1-Cre expression (red) at this age is ubiquitously expressed throughout the entire brain and other regions of the embryonic head ($n = 3$). (*E*) Coronal brain section of an E13.0 *ephrinB1*$^{lox/+}$;*ephrinB2*$^{loxp/loxp}$ cKO embryo containing the FoxG1-Cre driver allele. These cKO embryos also have normal TCA axon wiring at this early age ($n = 3$) demonstrating that a single copy of ephrinB1 is sufficient for proper TCA axon development, and that ephrinB2 in VTel is not necessary for the proper guidance of these axons. (*F*) Control brain section of an *ephrinB1*$^{+/+}$;*TetO-tdTomato* reporter embryo at age E13.5 that is clear of nonspecific tdTomato fluorescence. (*G*) Combined graphical representation of VTel misprojection scores from FoxG1-Cre driven ephrinB1 (both male *ephrinB1*$^{loxp/Y}$ hemizygous and *ephrinB1*$^{loxp/loxp}$ homozygous females) and ephrinB2 cKO mutants at E13.0 outlined in Fig. 7 *B* and *C*, respectively, compared with *FoxG1*$^{Cre/+}$ controls. *$P < 0.05$, Fisher's exact test.

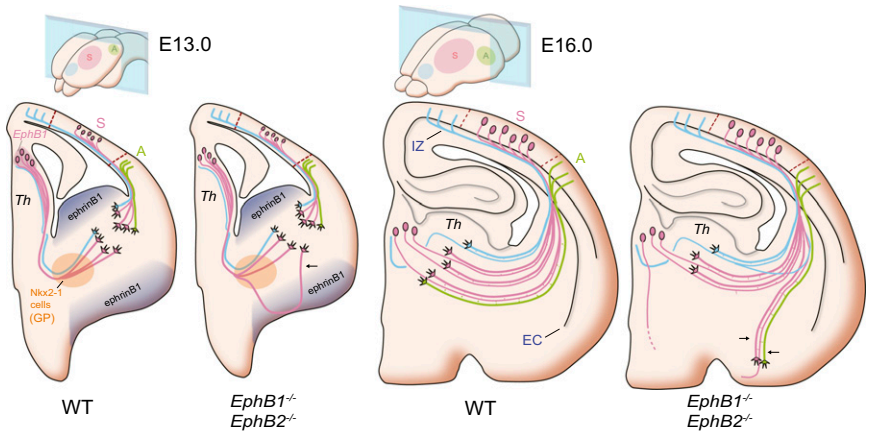

Fig. S8. Model of EphB1-dependent cortical and thalamic wiring in the VTel. Diagrams of cortical-thalamic wiring at embryonic age E16.0 in WT and *EphB1/2 DKO* conditions. A subpopulation of descending cortical fibers from the putative somatosensory cortex (pink S) and auditory cortex (green A) selectively cofasciculates along TCA misprojections that originate, in part, from the caudal thalamus where EphB1 is highly expressed.

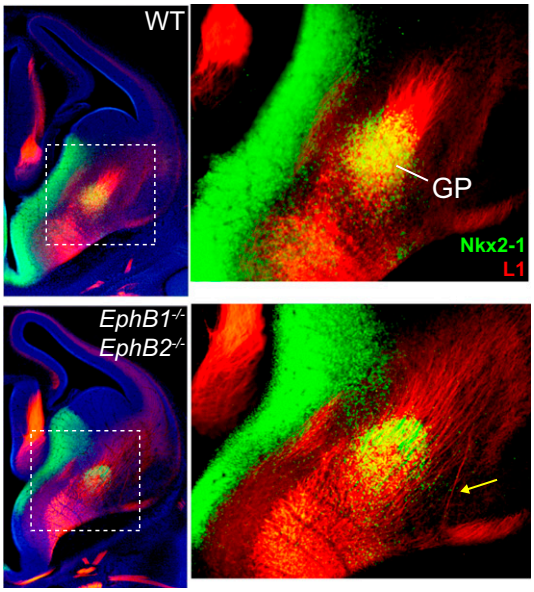

Fig. S9. TCA axons traverse the Nkx2.1 corridor in the VTel. E14.5 coronal brain section of a WT and *EphB1*$^{-/-}$*EphB2*$^{-/-}$ knockout mice that are dual-immunostained with anti–Nkx2-1 (green) and anti–L1-CAM (red). Nkx2-1–labeled cells (green) are localized in the GP regions of the VTel, and L1-CAM^{+} TCA fibers pass directly through this cell population (WT, $n = 2$; *EphB1/2 DKO*, $n = 4$). The L1-CAM^{+} misprojection in the *EphB1/2 DKO* mutant brain (arrow) is located lateral to the Nkx2-1–positive GP region.